Seismic imaging of thrust faults and structural damage: a visualization workflow for deepwater thrust belts

D. Iacopini,[1] R.W.H. Butler[1] and S. Purves[2] describe powerful analytical but simple-to-apply workflows for delineation of structural deformation in compressional folds imaged in 3D seismic volumes.

Combinations of increasingly sophisticated software and hardware have greatly improved the imaging of geologic structure and stratigraphic features in seismic datasets (Marfurt and Chopra, 2007). Today the seismic interpreter can quickly create attribute maps, using specific filtering workflows to identify, visualize, and isolate faults and fracture systems at different scales. Such techniques have been successfully applied for imaging normal faults (Dutzer et al., 2009) within reservoirs associated with extensional sedimentary basins (Chopra and Marfurt, 2007). However, most of the adopted interpretation strategies assume fault structures to be rather simple – represented as narrow curvi-planar surfaces that transect the seismic data.

This simplification implicitly assumes that deformation has localized onto a few fault strands. Equivalent simplifying assumptions have been made in the compressional toe-slope structures on deepwater slopes. Structural interpretations routinely opt for one of a narrow range of models that relate stratal anticlines to individual thrust faults (so-called 'end-member models'). However, high quality 3D seismic data show that the deep-water anticlines typically display complex variations in along-strike fold morphology which are not predicted by any individual fold-thrust model (Higgins et al., 2009). Furthermore, while the 'end-member models' are used routinely in academic publications, results from an expert-elicitation study have shown that experienced industry-based interpreters tend not to use these models when identifying faults (Torvela and Bond, 2011). The more complex models of thrust zone architectures used by the expert group accord with fault patterns seen in outcrop examples (Butler and McCaffrey, 2004; Braathen et al., 2009). These different models of thrust zones and related deformation have significantly different implications for fluid transmissivity. Yet even in very high quality 3D seismic data, critical parts of the thrust anticline structures are commonly represented by wipe-out zones (e.g. Kostenko et al., 2007). Consequently, image enhancement approaches are needed to resolve thrust zone structure. In a companion paper (Iacopini and Butler, 2011) we introduced a method of using seismic attributes to identify the geometry of complex thrust zones and associated structural damage. Here we develop the techniques into workflows for image processing, and the structural interpretation of these images, that combine seismic attributes through volume visualization techniques to describe and map volumes of deformed strata at the seismic resolution of 10s to 100s m.

Background

Defining the geometry of faults and distributed deformation is a serious challenge using even high quality 3D seismic data. Our approach here is to identify and delineate volumes of disturbed seismic signal. We term these seismic disturbance zones (SDZs). One widely-used approach for fault mapping in 3D data is to identify stratal breaks on selected 2D views, vertical profiles, and time/depth slices, and pick these as fault sticks. Here we use the entire volume, visualized in 3D, to investigate the amplitude, phase, and time attributes of SDZs. The range of seismic attributes increases the information used to deduce rock properties in the SDZs. Working in 3D improves the interpretation and is time-efficient. Sub-volumes may be selected for further, detailed treatment. The 3D visualization tools allow the interpreter to rapidly evaluate structural relationships, significantly enhancing the understanding of features otherwise observed in 2D profiles or maps.

The seismic dataset used here to illustrate the workflow is from the outer zones of the deepwater Niger delta. It comes from the multi-client library of CGGVeritas and in common with many other deepwater settings, is of very high quality. The data are from a post-stack volume, processed via a fully ray-traced Kirchhoff pre-stack time migration. The relative vertical resolution is estimated at around 5–50 m

[1] *Geology and Petroleum Geology Department, University of Aberdeen, UK.*
[2] *ffA, Newcastle upon Tyne, UK.*
[*] *Corresponding author, E-mail: d.iacopini@abdn.ac.uk*

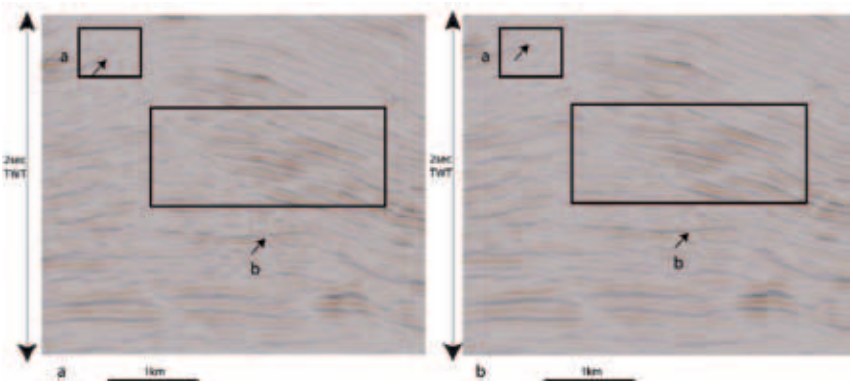

Figure 1 *The effect of noise cancellation filters on seismic data, displayed in amplitude, extracted from a 3D cube. a) Shows the state before the noise cancellation; b) Shows the enhanced data quality after the application of the noise cancellation filter. The arrow identifies a detail of the noise filtering. Note how the incoherent signal in (b) and in (a) has been sharpened and enhanced after the noise cancellation for this arrowed feature.*

depending both on the dominant frequency within the depth of interest (from 60 to 5 Hz) and on the mean stack velocity (from 1.5 m/s to 3.6 m/s, Morgan, 2003) The seismic data are displayed here in TWT.

On a large-scale, the geological structure of the outer part of the toe-thrust system of the Niger delta is uncontroversial. The upper 3–4 km of the sedimentary pile consists of turbidite sandstones and associated mud-rocks (the Akata Formation) that have decoupled from the underlying oceanic crust by a sheared, over-pressured mud-rock sequence (the Agbada Formation). Above this detachment zone, the Akata Formation has developed a series of contractional folds and related thrusts (Higgins, 2009). It is the detailed arrangement of deformation within these fold-thrust structures that forms the focus of our study. We concentrate on a single thrust-cored anticline.

We then address the description of the post stack seismic analysis with the overarching aims first to improve image quality and subsequently to interpret the structural geology. We use opacity, structural oriented filters, different volume attribute extraction techniques (e.g., semblance, curvatures, and spectral decomposition) and visual correlation methods (volume rendering and blending techniques). We propose our proprietary Geological Expression workflow using GeoTeric to investigate thrust and fault structures in general and suggest possible structural interpretations of the seismic disturbance zones.

Geological Expression workflow

The analytical workflow applied in this study utilizes seismic data containing faults resulting in the development of a thrust fault workflow which features robust algorithms and advanced visualization techniques especially suited for the expression of geological features within thrust and fault belt data sets.

The workflow consists of:

1. Noise cancellation
2. Structural and fault imaging using dip and semblance map
3. Frequency decomposition
4. Curvature analysis
5. Curvatures/semblance cross plotting
6. Volume blending and rendering.
7. Definition and extraction of geobodies

One or more analytical algorithms are applied at each stage in the workflow. Each of these has parameters that allow them to be tuned to the particular characteristics of the dataset, the noise present, and the geological targets that are the subject of the analysis. These are now described in turn.

Step 1: Noise cancellation

A necessary step to improve 3D seismic data quality, prior to attribute analysis and interpretation work, is the removal of noise. This must be performed whilst minimizing the loss of information. Methods for attenuating both random noise and high spatial frequency coherent noise have been applied sequentially in this workflow. In this instance, we needed to achieve a high level of continuity along stratal reflector events whilst maintaining subtle details such fault breaks and significant variations in amplitude and we have tuned the filters accordingly.

In order to remove random noise and increase reflector continuity, an anisotropic edge preserving diffusion algorithm was used. This filtering operation takes the form of a diffusion operator that is defined by a partial differential equation (PDE), such as second order heat flow or Fick's Second Law. Fick's Second Law gives the rate of change of concentration due to diffusion by:

$$\frac{\partial u}{\partial t} = D\nabla^2 u$$

If we take u to represent seismic amplitude and our 3D dataset as the initial conditions of those amplitudes, then this equation describes how those amplitudes should change over time in response to the diffusion process, defined here by the operator, D.

By applying this model, we are in effect iteratively solving the PDE over the dataset causing a 'flow' in amplitude from high to low values as the amplitude field becomes more diffuse overall. This is not a desirable effect on its own. So, in order to use such a model for noise reduction in 3D seismic data, two important modifications are made when solving the PDE.

Firstly, a tensor-based representation is used, implicitly allowing diffusion to be restricted to within the local surface

of the seismic reflector and not across it. In essence, the filter becomes 'dip compensated' or 'dip steered' where the local reflector dip is automatically calculated as part of the filtering operation. Secondly, the diffusion tensor D, is modified so as to add coherence-preserving behaviour, which alters the spatial region of support of the operator in the presence sharp amplitude changes. This tends to preserve and in some cases reinforces reflector breaks (e.g., due to faulting and subtle structural features). The main reflectors are enhanced and smoothed as well (arrows and square in Figures 1a and b).

The diffusion operator preserves major structural discontinuities, reflector terminations and faults. The iterative nature of the operation and the ability to affect the rate of local diffusion mean it is possible for the interpreter to exercise a significant amount of control over the degree of noise reduction and the amount of level of structural detail preserved.

This dataset contains volumes that are affected by high frequency coherent noise. This cuts across reflectors and is more evident and troublesome in regions of greater reflector dip.

Step 2: Structural oriented filtering and fault imaging

This is the process of generating volumetric seismic attributes that highlight and emphasize geological structure and aid the detection of areas of deformation associated with faulting. Important measurements in this category are dip and azimuth. In the first instance, we compute the dip and azimuth of structures within the noise-cancelled source data volume. We use the so-called 'phased-based option' that utilizes the structural phase, rather than the amplitude, of the seismic trace to calculate the dip and azimuth at each voxel. The SVI software allows dominant orientations to be computed at a range of scales and, whilst larger scale estimated have been used as steering volumes within the noise cancellation step, the finer and correspondingly more detailed volumes are generated for use in structural interpretation. These steering volumes are created by examining the local phase signal at every voxel within the dataset and can be parameterized to capture local, correspondingly small scale variations or smoother, more generalized estimates of structural orientation. The generalized orientation estimates are less sensitive to the presence of faults and discontinuities in the data and thus are the most useful for steering the filter. The filter uses these orientation estimates to align itself with a 2D platelet of seismic amplitudes within the local reflector structure, to which the filtering operation is subsequently applied.

Structure-oriented filtering must be performed so as to identify and possibly differentiate the main dip azimuth of the reflector from the overlying noise. A median hybrid structurally oriented filter is applied to do this. This filter exhibits two important properties that account for its ability to deal with coherent noise. Firstly, the filter is driven by external dip and azimuth volumes that estimate the orientation of local structure. The second important property is a consequence of how the filter kernel is constructed. Here the 2D platelet, $\boldsymbol{x}$, is split into sub regions, $\boldsymbol{x}$k, the geometry of which is carefully chosen to promote edge and detail preservation.

The kernel applies multiple median operations in cascade in order to compute a new seismic amplitude value for each voxel in the data. An example of a cascaded median configuration would be:

$$y = med\{med\{x_n\}, med\{med\{x_1\}, med\{x_2\}, med\{x_3\}\}, med\{med\{x_4\}, med\{x_5\}, med\{x_{63}\}\}$$

This produces a filter that is good at preserving structural detail within the 3D seismic dataset whilst recognizing and attenuating coherent noise. The user can tune the filter to maximize removal of the coherent noise whilst maintaining as much structural detail as possible.

The volume dataset obtained so far is called conditioned volume dataset and it forms the starting point from which to apply the main geometric and amplitude seismic attributes (semblance, curvatures, frequency decomposition).

Highlighting faults – semblance: At this stage of the process, attention can be focused on the major discontinuities and incoherencies within the volume dataset which might correspond to structural faults and broader volumes of structural damage. A type of coherency algorithm is employed that uses the well-known semblance multi-trace correlation calculation (Marfurt et al., 1998) to identify discontinuities and reflector distortions within the data. The multi-trace semblance algorithm provides an improved vertical resolution with respect to the original and classical normalized cross-correlation algorithm of Bahorich and Farmer (1995), as it no longer requires an analysis window that is greater than the longest period in the data, minimizing vertical smearing of geologically relevant information. Semblance can also use a larger number of traces increasing the stability of the filter and its tolerance to noise.

The algorithm used improves further on standard coherency and semblance-type algorithms (Marfurt et al., 1998) by adapting to local dip to ensure that the semblance measure is taken in the pole direction of the reflector. It is important that the algorithm carefully analyses structural and stratigraphic features over the entire volume identifying subtle features that are not merely represented by peaks, troughs, or zero crossings alone.

Scale may be defined by the number of traces (X, Y) included in the calculation in each direction together with the trace length used. The scale needs to be chosen so that it is large enough to 'see' across those faults or discontinuities that will be considered later in the workflow. The outputs of this computation are volumes that highlight not only coherent regions of data but also individual faults and broader incoherent regions. In our study it is the latter that

have been used to great effect for delineating and interpreting volumes of the structural damage (Figure 2). Note the complexity and anastamosing geometry of the fault and thrust zones (damage zones, 1 to 3 in Figure 2) that define the principal deformation structures in this part of the fold-thrust structure (for a detailed discussion on the nature of the discontinuities observed, see Iacopini and Butler, 2011). In particular, the attribute obtained from the SOS has been further processed with smoothing filters to improve the vertical and lateral continuity within the major fault damage zones. As described below, this allows these regions to subsequently be extracted as geobodies and their geometry in 3D to be examined in detail. We now focus on some specific parts of the data volume to explore the main properties of selected disturbance zones (denoted by arrows in Figure 2).

Step 3: Frequency decomposition

Frequency Decomposition is achieved through application of a bank of band-pass filters are used to target frequencies of interest within the data. The filter kernel is based on a 1D Gabor wavelet function and is applied in the seismic trace direction. The Gabor wavelet is used as it optimizes time-frequency resolution when attempting to localize frequency information within a band-limited data set such as a 3D seismic volume.

This decomposition technique is used to examine and compare the frequency content of our data at different frequency bands using a Red–Green–Blue (RGB) blending scheme. The results are virtual RGB seismic attribute cubes that can then be visualized in 3D. In essence, RGB blends combine information provided by three input images to generate a single full-colour output image. This in turn allows image properties to be retained in regions of homogeneous behaviour while bringing out variations in those properties away from homogenous areas.

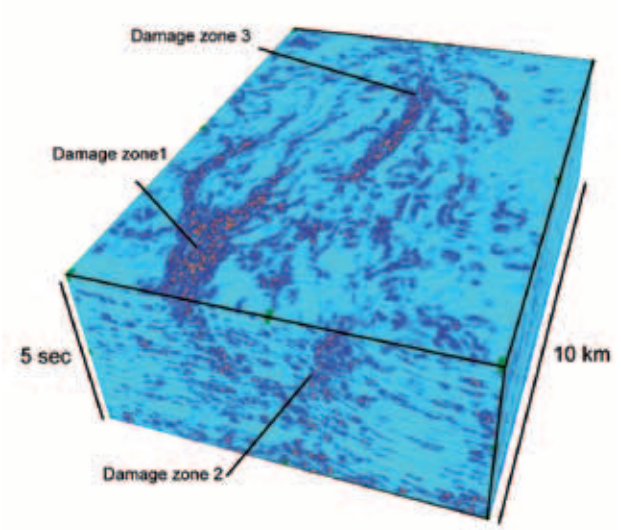

Figure 2 *Main seismic damage zones identified by the semblance volume of coherencies.*

RGB blending is a well-known technique, however in this study we have applied a CMY blending model that works on the same principles as RGB blending. The CMY (Cyan–Magenta–Yellow) model is a subtractive colour alternative to RGB that is useful in visualizing structural elements and their variation in character.

The quality of an CMY-blended image is dependent on the available colour resolution. In this work, the CMY blend has been created with an 18-bit colour resolution (262,144 colours) where six bits are assigned to each of the input channels (Cyan, Magenta and Yellow).

We find that the resulting outputs can be visually assimilated rapidly by an interpreter. The workflow applied comprises the following steps:

1) Selection of the sub-volume data
2) Selection of the frequency decomposition parameters ensure that the bandwidth of each filter channel is constant
3) Selection of the responses at three frequencies of interest (in this case 13Hz, 38Hz and 55 Hz) to combine in the CMY blend
4) Visualization and interpretation of the resulting multi-attribute volume (Figs 3 a to d)

The key difference in the workflow applied here is in the source dataset. Usually the frequency decompositions are applied to seismic volumes represented in amplitude. As we are attempting to characterize the faulted zones within the dataset we have applied the frequency decomposition workflow (Figure 3) to the structure-oriented semblance attribute itself, rather than the original reflectivity data. While being a valid operation, the results require a very different interpretation to conventional approaches. Figure 3 shows that despite the variability of the main thrust and damage zones imaged, the main discontinuity and damage zones are preserved across the different frequencies. A CMY blend volume that associates a different colour to each frequency-dependent feature allows us to produce a map of the tuning thickness (in Step 6 below). This highlights the distribution of the main features through frequency within damage zones. As such it shows that the main discontinuities and damage zones are represented through the entire bandwidth range, thereby discriminating real geological structures from seismic artifacts that are restricted to specific narrow frequency bands.

Step 4: Volumetric curvature

These attributes are created using an algorithm that examines the first derivative of dip. This picks up faults or structures that are expressed not as discontinuities but by seismic distortions such as folds, flexures, and associated high curvatures. Note that curvature is not computed in the strict sense. Rather, the algorithm examines the directional rate of change in the maximum structural dip to generate a

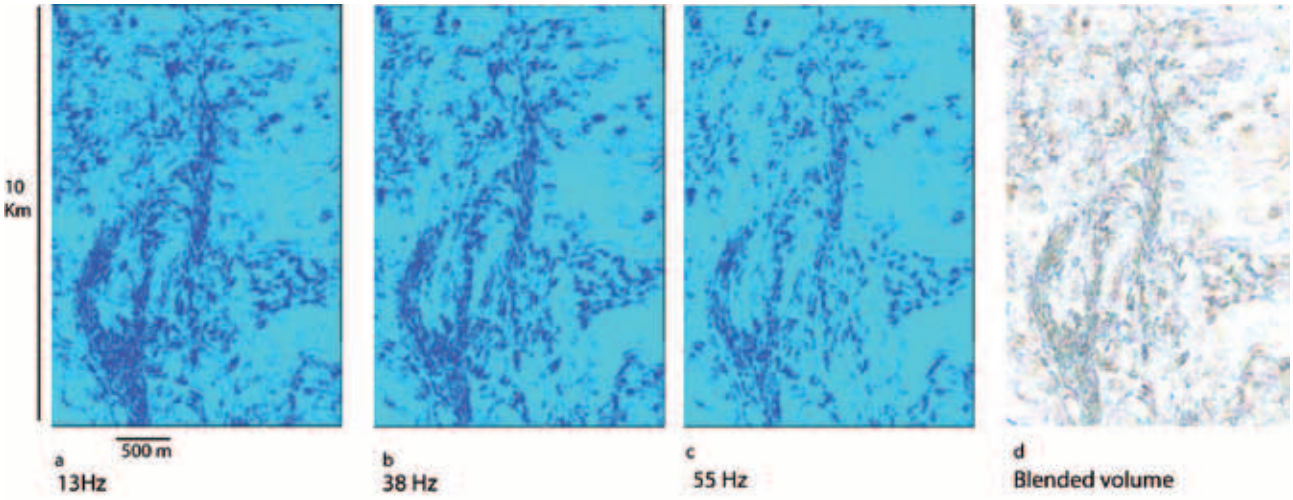

Figure 3 *Comparison at different frequency peaks illustrated on an arbitrary time slice at 5.9 s TWT. a) Discontinuities extracted from the regional semblance cube in Fig. 3 at discrete frequency of 13Hz. b) time slice at a discrete frequency of 38 Hz. c) time slice at a discrete frequency 55 Hz. d) CMY blend highlighting the relationship between the main disturbance bodies at different frequencies.*

directional measure of the second partial derivative of the original noise-cancelled seismic data.

By using a small-scale neighbourhood (defining the number of neighbouring voxels to be examined around each point) it is possible to obtain a detailed computation of the positive (convex-upwards) and negative (concave-upwards) curvature across the volume dataset. These values relate to the geological structure, with antiforms (upward-closing folds) seen as positive (blue) and synforms (downward-closing folds) seen as negative (red: Figure 4) By utilizing colour co-rendered visualization, the curvature volumes can be combined visually with an arbitrary vertical dip-profile from the original dataset (displayed in amplitude). This highlights that the thrust-cored structures are associated with the majority of the positive and negative curvatures.

In this study we are interested in how discontinuities and curvatures to larger scale structure. We achieve this by co-rendering, again within a CMY blend, structural dip (cyan), flexure (magenta), and structurally oriented semblance (yellow) attributes.

The resulting multi-attribute volumes are especially useful in identifying how low semblance regions relate, on the one hand to the larger dislocations and fault strands (green on Figure 5) and on the other hand to probable regions of distributed to strain (yellow on Figure 5). The major discontinuity and perturbance zones are clearly visible in the volume while variations in magenta shows the large scale curvatures associated with the major fold structures. This highlights that the thrust core fault like structures are aligned with the distribution within the 3D semblance volume in Figure 2.

Step 6: Cross-plotting attributes

Cross-plotting is a technique that provides a visual means for an interpreter to see trends and correlations between mathematically-independent measures that are correlated through the underlying geology. This technique has been routinely used both for AVO analysis and for defining faults and fractures (Chopra and Marfurt, 2009). Here the cross-plotting method is applied to denote deformation within the limbs of the major fold structure. Curvatures (which measure part of the structural deformation) and coherence (which measures waveform discontinuity) are mathematically-independent attributes that can be cross-plotted to identify volumes where the strain is especially localized (Figure 6a).

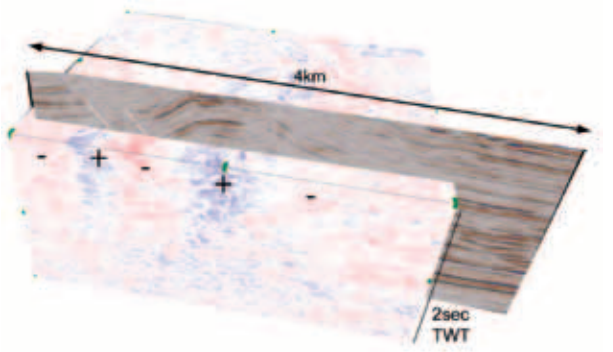

Figure 4 *Positive and negative volume curvature displayed with a vertical section of a seismic amplitude volume. Note that the positive (blue) and negative (red) curvatures are associated with the main synform and antiform of the major thrust-related fold.*

As shown in Fig 6b, the cross-plot of coherence against the most-positive curvature defines a bell-type distribution of points. Polygon (a) in Figure 6b identifies faults that are associated in clusters with low coherence and high most-positive curvatures (yellow polygon in Figure 6b). Regions of distributed strain within the fold are associated most obviously to patches of low semblance and with both the lowest and highest curvatures (green polygon and related green zones in Figure 6a). These patterns may be compared

with the clusters associated with zero curvatures and low coherencies (red polygon in Figure 6a). These do not appear to relate to offsets of stratal reflectors (mappable faults) or to hinge lines of the major fold. Rather, they may represent distributed strain containing arrays of deformation structures (e.g., small faults, tracts of fluid-filled fractures) that lie below the resolution of the 3D volume. Thus the cross-plotting approach provides a means of separating different types of deformation. As described below, these zones can be then extracted and sculpted as volume geobodies.

Step 7: Defining disturbance geobodies

There are a number of ways to extract, manipulate, and analyse geological elements, which have distinct characteristics expressed on one or more of the seismic attributes. The resulting 3D geometries are known as geobodies. The key to successful extraction of useful geobodies, is to properly invest in imaging the geological elements of interest via seismic attribute processing. These steps require intervention and the results are therefore dependent upon the decisions taken by the interpreter.

Three fundamental steps are needed to generate geobody volumes that can be used as an interpretation aid, starting from an appropriate attribute cube.

Body labelling is a process used to extract and analyse connectivity between geological elements to produce independently-labelled 3D geobodies. (Figure 7a). Once this selection is made, a connectivity analysis is run, and various criteria are applied not only to constrain the degree of connectivity used but also to filter target geobodies based on size. Once the initial geobodies are defined, body morphology filters are applied for further refinement.

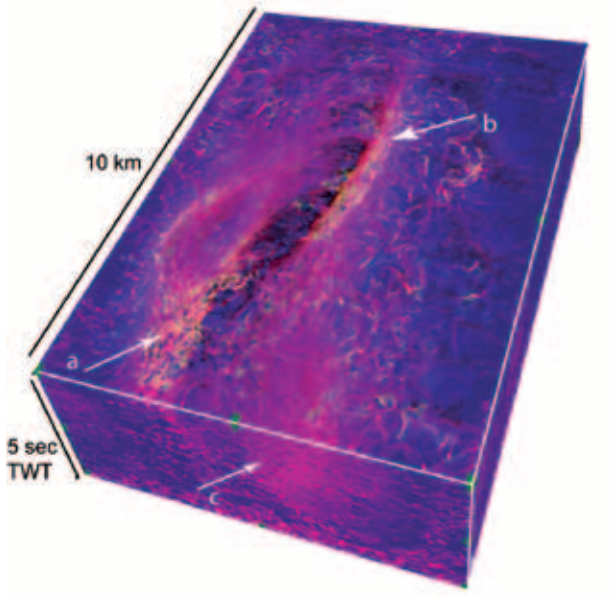

Figure 5 *CMY blend highlighting the relationship between dip, incoherency, and positive curvatures associated with the main damage zones.*

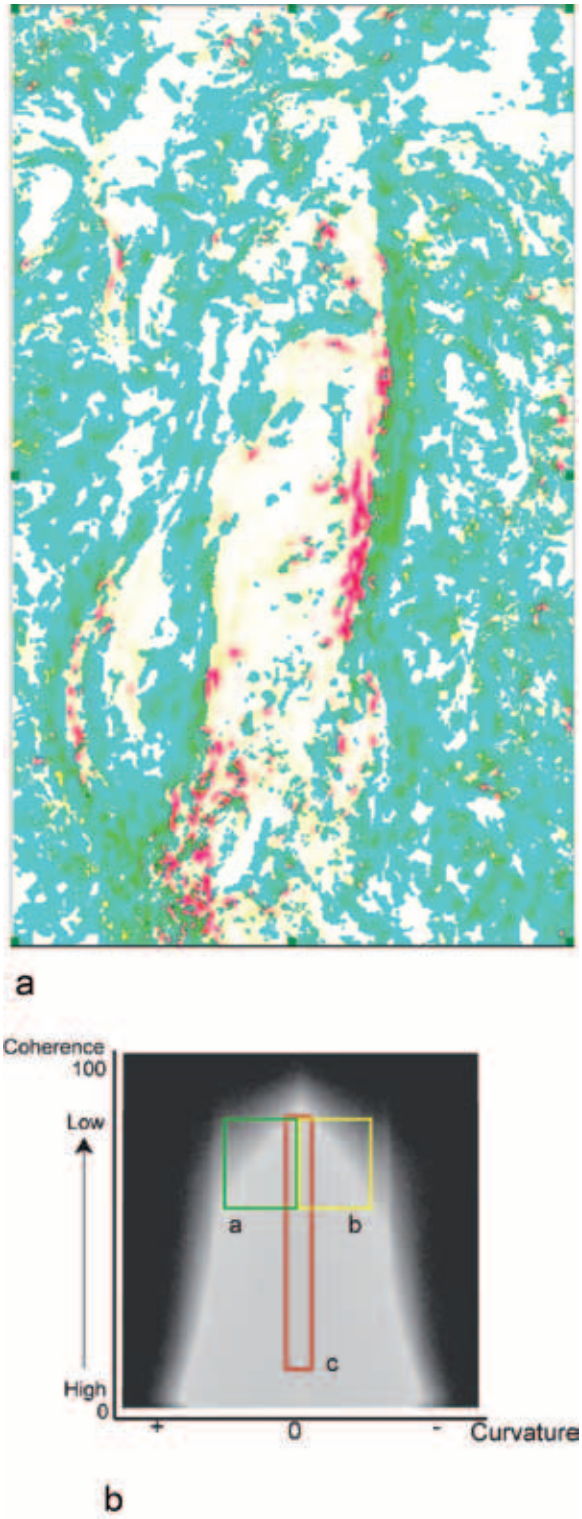

Figure 6 *a)Arbitrary time slice extracted from the CMY blend derived from blending cross-plots cluster point from red, yellow, and green polygons. b) Cross-plot of coherence versus curvature (positive, zero, and negative). The polygons are respectively shown in green, red, and yellow cluster points with the positive, zero, and negative curvatures associated to the low semblance zones. This volume blend highlights a variety of strain features within the damages zones.*

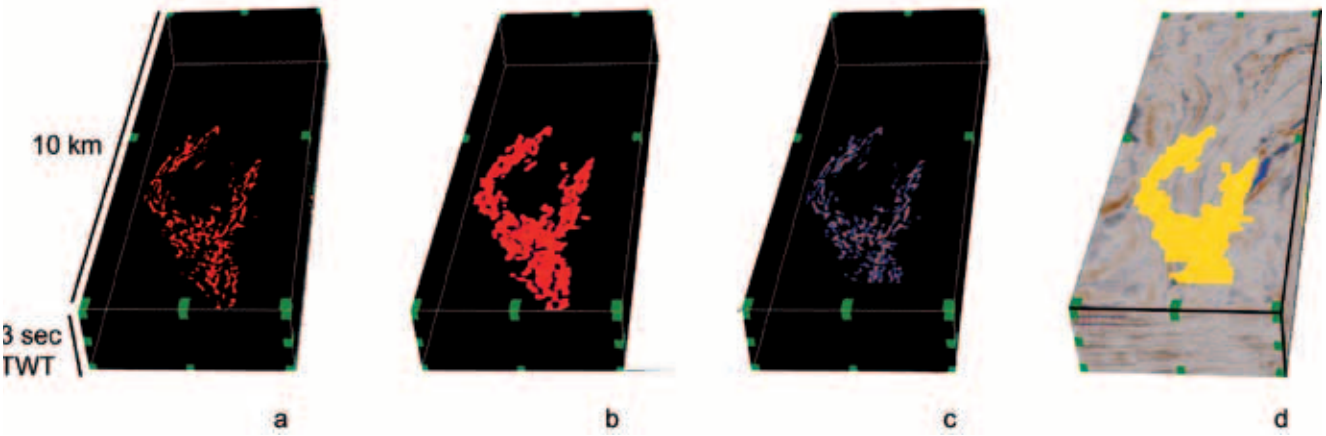

Figure 7 *Geobodies derived from: a) body labelling; b) body morphology filter; c) labelled bodies re-populated with incoherency attributes; d) cookie cutter used to embed back the geobodies into the original dataset.*

Body morphology (a filter) is an interpretative tool that allows geobodies to be reshaped in a data-driven manner, subtly smoothing their boundaries, opening and closing holes and connecting or disconnecting bodies based on apparent strength of the original connection between them (Figure 7b). Previously labelled bodies can be re-populated with data from an attribute volume to investigate how this attribute varies within the geobody (Figure 7c).

Finally, the geobodies can be collected and embedded back within the reflectivity cube for subsequent examination and interpretation (Figure 7d). These types of 'cookie-cut' volumes are very powerful visual aids and help in understanding how 3D geometries of the fault zones relate to other structural and stratigraphic elements within the data. Applying this step in the workflow allows us to obtain the volume in Figure 7d.

By applying volume rendering and a colour-code (red and green) according to their geological relationship disturbance, geobodies can be visualized and pasted into the original 3D dataset. In Figure 8 the colour green is used to designate geobodies developed on the back-limb of the major fold. These are not associated with mappable discontinuities and therefore are interpreted to represent volumes of distributed structural damage. In contrast, geobodies associated with thrust discontinuities in the forelimb of the major fold are coloured red. These volumes may represent thrust-related damage and shearing. The main thrust discontinuity obtained from the conventional picking of the fault (green surfaces) can be pasted back thereby providing a useful volume for the investigation of the damage zones and eventually the quantification of the volume of probable structural damage and concomitant risk to reservoir quality.

Discussion and conclusion

The analytical workflow is powerful but simple-to-apply workflows for delineation of structural deformation in compressional folds imaged in 3D seismic volumes. In particular, advanced multi-volume visualization techniques improve the understanding of the relationships between tracts of structural distributed deformation, broader thrust damage zones, complex thrust splays, and the larger-scale fold-thrust structure. These in turn could be used in the future to develop better understanding and definition of the damage within and adjacent to reservoirs. Geobody characterization using seismic attributes and their cross-plotting can greatly aid 3D seismic interpretation of structural features associated with reservoir and caps rock within deep water thrust systems. Cross-plotting allows us to interactively cluster the attributes to enhance recognition of those deformation features of interest. This can be achieved not only at a regional scale but also at a more detailed prospect level scale. Such workflows save considerable time and effort by avoiding the laborious task of conventional interpretation on individual profiles in the 3D volume.

Clearly the structural interpretations made here are provisional and in an exploration or development setting would

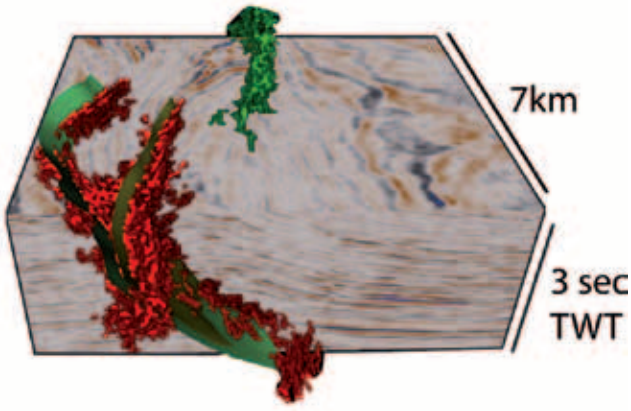

Figure 8 *Final rendered geobodies pasted on the initial volume dataset. Represented in red are the disturbance geobodies associated with the main thrust and fault discontinuity zones. Represented in green are the main disturbance geobodies associated to the distributed strains (i.e., without an independently-mapped discontinuity surface) on the back-limb of the major fold.*

await confirmation from well penetrations. Nevertheless, the workflows developed here may help to reduce risk in these challenging settings.

Acknowledgements

We thank Steve Toothill and colleagues from CGGVeritas for permission to work and publish on the 3D dataset from the Niger Delta. Images presented here are also available within the Virtual Seismic Atlas (www.seismicatlas.org). The work has been supported by University of Aberdeen (College of Physical Sciences) research funds. We also thank ffA for provision of their software to the University of Aberdeen.

References

Braathen, A, Tveranger, J., Fossen, H., Skar, H., Cardozo, N., Semshaug, S.E., Bastesen, E., Sverdrup, E. [2009] Fault facies and its application to sandstone reservoirs. *AAPG Bulletin*, **93**, 891–917.

Butler, R.W.H. and McCaffrey, W.D. [2004] Nature of thrust zones in deep water sand-shale sequences: outcrop examples from the Champsaur sandstones of SE France. *Marine and Petroleum Geology*, **21**, 911–921.

Chopra S. and Marfurt, K.J. [2009] Detecting stratigraphic features via cross-plotting of seismic discontinuity attributes and their volume visualization. *The Leading Edge*, **28**, 1422 –1426.

Dutzer, J.F., Basford, H., and Purves, S. [2009] Investigating fault sealing potential through fault relative seismic volume analysis. *Petroleum Geology Conference* series, **7**, 509–515, doi:10.1144/0070509.

Henderson, J., Purves, S. and Leppard, C. [2007] Automated delineation of geological elements from 3D seismic data through analysis of multi-channel, volumetric spectral decomposition data. First Break, 25(3), 87–93.

Higgins, S., Clarke, B., Davies, R.J. and Cartwright, J. [2009] Internal geometry and growth history of a thrust-related anticline in a deep water fold belt. Journal of Structural Geology, 31, 1597–1611.

Iacopini, D. and Butler, R.W.H. [2011] Imaging deformation in submarine thrust belts using seismic attributes. *Earth Review Planetary Science Letter,* in press

Kostenko, O.V., Naruk, S.J., Hack, W., Poupon, M., Meyer, H.J., Mora-Glukstad, M., Anowai, C., Mordi, M. [2008] Structural evaluation of column-height controls at a thrust discovery, deep water Niger Delta. AAPG Bulletin, 92, 1615 –1638.

Marfurt, K.J. and Chopra, S. [2007] Seismic attributes for prospect identification and

reservoir characterization. SEG Geophysical development (11).

Marfurt, K.J., Kirlin, S.H., Farmer, S.H. and, Bahorich, M.S. [1998] 3D seismic attributes using a semblance based algorithm. Geophysics, 63, 1150 –1165.

Marfurt, K.J, Sudhakar,V., Gersztenkorn, A., Crawford, K.D. and Nisse, S.E. [1999] Coherency calculations in the presence of structural dip. Geophysics, 64, 104 –111.

Torvela, T. and Bond, C.E. [2011] Do experts use idealized models? Insights from a deepwater fold-thrust belt. Journal of Structural Geology, 33, 51–58